# Inhibition and promotion of an isothermal flame in the low-pressure thermal decomposition of nitrogen trichloride

**Nikolai M. Rubtsov*[a] and Vyacheslav D. Kotelkin[b]**

[a] *Institute of Structural Macrokinetics and Materials Science, Russian Academy of Sciences, 142432 Chernogolovka, Moscow Region, Russian Federation. Fax: +7 095 962 8025; e-mail: ab3590@mail.sitek.ru*
[b] *Department of Mechanics and Mathematics, M. V. Lomonosov Moscow State University, 119992 Moscow, Russian Federation. Fax: +7 095 939 2090; e-mail: kotelkin@mech.math.msu.su*

10.1070/MC2002v012n06ABEH001630

The inhibition and promotion of an isothermal flame by NOCl and $H_2$, respectively, are considered based on a kinetic mechanism taking into account energy chain branching.

Previously, we reported the numerical simulation of some kinetic features of the branching chain process (BCP) of nitrogen trichloride ($NCl_3$)[1–3] decomposition due to nonlinear steps in the BCP mechanism. Unlike hydrogen oxidation, which is a model BCP governed by linear chain branching, $NCl_3$ decomposition is controlled largely by the positive chain interaction (reaction in which the number of free valences increases as a result of the interaction of active centres[4]). This phenomenon gives rise to structural-organization effects, namely, isothermal flames[5–8] and chemical oscillations.[9] The experimental data on self-ignition, oscillating regimes, velocities and limits of isothermal flame propagation (IFP) in various diluents and a transition from IFP to a chain-thermal flame propagation were examined[1–3] on the basis of a kinetic mechanism including energy chain branching.[5,6] In all cases, the experimental and calculated data were in qualitative agreement. The region of IFP is much broader than the autoignition region.[4] Therefore, because of the high fire hazard, special precautions should be taken in carrying out BCP with nonlinear steps. This is particularly true for industrially important reactions such as silane oxidation and electrolytic chlorine production, where $NCl_3$ is a by-product.[10,11]

The branching chain mechanism, which means competition between chain branching and termination, is a crucial factor in gas-phase combustion between a few Torr and super atmospheric pressure.[12] Because the temperature rise, which accelerates branching chain reactions, results from this reaction, combustion can be effectively controlled by chemical means. In view of this, it is essential to develop flammability control methods for nonlinear BCP, in which a radical avalanche can form at a combustible-substance concentration below 1%.[4,5] Thus, it is very important to study the inhibition and promotion of isothermal flames by active chemical additives. A study of $NCl_3$ decomposition in the presence of inhibitors and promoters is relevant to both explosion safety in chlorine industry and the use of $NCl_3$ in laser chemistry.[13]

We consider the effects of inhibition and promotion on the IFP in dilute mixtures of $NCl_3$ in the presence of NOCl (inhibitor) or $H_2$ (promoter), taking into account the energy branching of chains.[1–9] Earlier, we reported the inhibition of $NCl_3$ decomposition by NOCl[8] and the promotion of this process by $H_2$.[6,14] The possibility of inhibiting IFP was considered in terms of a generalised kinetic scheme.[15]

The experimental procedure was described elsewhere.[3,5,6] Self-ignition limits were determined in a heated quartz reactor 20 cm in length and 6 cm in diameter. The inner surface of the reactor was covered with MgO, which provides the diffusive area of chain termination.[8] To study inhibition, pure NOCl was admitted into a heated prepumped reactor. Next, an $NCl_3$–He mixture was added, and the reactor was allowed to stand for 5 min for perfect mixing. In promotion experiments, nitrogen trichloride was evaporated into hydrogen.

Figure 1 illustrates experimental data on the inhibition of IFP in $NCl_3$ by NOCl. As the inhibitor concentration is increased, the maximum flame velocity $U$ decreases, the lower IFP limit rises, and the upper IFP limit decreases. It is noteworthy that the $U$ value at the upper IFP limit is virtually independent of the inhibitor concentration at a constant $NCl_3$ concentration. Figure 2(*a*) presents experimental data illustrating the promotion of the IFP of 0.5% $NCl_3$ in $H_2$. For comparison, Figure 2(*b*) shows experimental flame velocity for helium containing 0.4 or 0.11% $NCl_3$.[2] A specific feature of the pressure dependence of the flame velocity in $H_2$ [Figure 2(*a*)] is that the upper IFP limit is not observed up to 500 Torr. The ratio between the diffusion coefficients of a probe particle in helium and hydrogen is ~0.9.[16] The velocity of an isothermal flame is approximately equal to the square root of the diffusion coefficient of the active centre involved in positive chain interaction.[4] It is clear from Figure 2 that, throughout the pressure range examined, the flame velocities in He and $H_2$ differ by a factor greater than $0.9^{1/2}$.

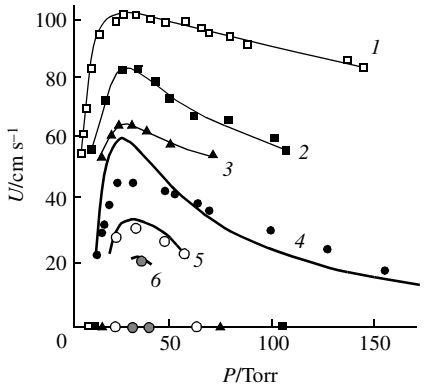


**Figure 1** Flame velocity in $NCl_3$–He mixtures (*1*), (*4*) in the absence and (*2*), (*3*), (*5*), (*6*) in the presence of NOCl as a function of total pressure. [$NCl_3$] = (*1*)–(*3*) 0.8 and (*4*)–(*6*) 0.23%; [NOCl] = (*1*), (*4*) 0, (*2*) 0.024, (*3*) 0.041, (*5*) 0.02, and (*6*) 0.025%. The points represent experimental data; the thick solid lines show data calculated for model (I); and the thin solid lines are least-squares fits to experimental data.

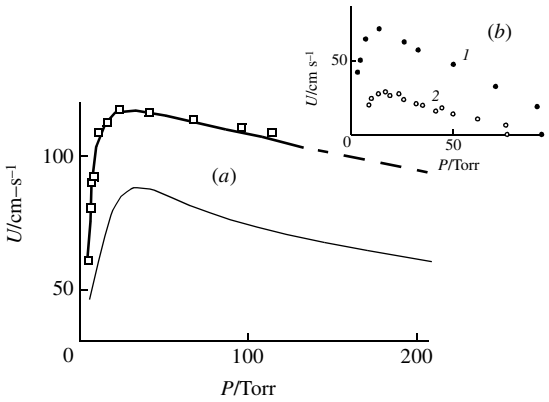


**Figure 2** Flame velocity as a function of total pressure: (*a*) $NCl_3$ (0.5%)–$H_2$ mixture (the points represent experimental data;[6] the thick line shows data calculated with allowance made for promotion; the thin line represents data calculated with allowance made for $H_2$ raising the diffusion coefficients of the intermediates without promoting $NCl_3$ decomposition) and (*b*) $NCl_3$–He mixture with [$NCl_3$] = (*1*) 0.4 and (*2*) 0.11%.[6]

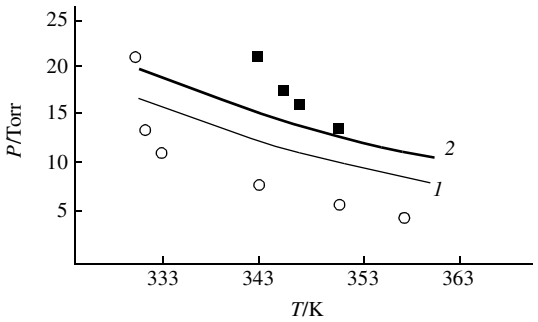


**Figure 3** Temperature dependence of the lower autoignition limit for (*1*) $NCl_3$ (0.5%)–$H_2$ and (*2*) $NCl_3$ (0.4%)–He mixtures. The points and lines represent experimental and calculated data, respectively.

Figure 3 shows experimental flammability limits for $NCl_3$–He and $NCl_3$–$H_2$ mixtures. Flame propagation in the $NCl_3$ (0.5%)–$H_2$ mixture occurs outside the self-ignition region; that is, the flame observed in this mixture is isothermal (the measured temperature rise does not exceed a few Kelvins[14]). Note that the lower self-ignition limit $P_1$ for $H_2$ is lower than that for He. The reverse situation would be observed without a promoting effect because heterogeneous chain termination takes place in the diffusion-controlled region of chain termination, and the diffusion coefficient of a probe particle in $H_2$ is higher than that in He. Therefore, $H_2$ promotes $NCl_3$ decomposition in both autoignition[17] and IFP regions. Raising the $NCl_3$ concentration in He widens the pressure range in which IFP is observed [Figure 2(*b*)]. We will demonstrate that, at the upper flame-propagation limit (0.4% $NCl_3$, 70 Torr), the temperature rise $\Delta T$ is insufficient for self-ignition. The minimum self-ignition temperature is 333 K (Figure 3). Therefore, if the mixture is initially at 293 K, the minimum temperature rise $\Delta T_{min}$ must be greater than 40 K. Let us refer to the relationship $\Delta T = QsP\times3\times10^{16}/(C_p\rho N)$,[18] where $C_p$ = 1.25 cal g$^{-1}$ K$^{-1}$ is the molar heat capacity of the $NCl_3$–He mixture,[19] $P$ is the total pressure (Torr), $s$ is the mole fraction of $NCl_3$ in the initial mixture ($[NCl_3]_0 = sP$), $N = 6.02\times10^{23}$ mol$^{-1}$, $\rho = 1.8\times10^{-4}$ g cm$^{-3}$ is the density of helium at 760 Torr,[19] and $Q$ = 60 kcal mol$^{-1}$ is the heat of the reaction $NCl_3 \rightarrow 1/2N_2 + 3/2Cl_2$.[20] Hence, $\Delta T \sim 5$ K $< \Delta T_{min}$. This means that the upper flame-propagation limit is isothermal. The data calculated below are consistent with this inference. The chain-thermal flame propagation is clearly observed in $H_2$ containing 8% $NCl_3$. In this case, flame propagates along the reactor with an apparent velocity of 400 m s$^{-1}$ at 30 Torr and produces a characteristic sound.

Let us analyse experimental data on the IFP in terms of the known elementary reactions involved in $NCl_3$ decomposition. The kinetic mechanism of $NCl_3$ decomposition, including the steps occurring in the presence of $H_2$ (promoter) and NOCl (inhibitor), can be represented as follows;[1–3,5,6,8,9,17,21,22]

$Cl + NCl_3 \rightarrow NCl_2 + Cl_2 + Q_1$,
$k_1 = 1.6\times10^{-12}$ cm$^3$ s$^{-1}$ (chain propagation),[22]

$NCl_2 + NCl_3 \rightarrow N_2 + Cl_2 + 3Cl + Q_2$,
$k_2 = 3.4\times10^{-11}\exp(-\varepsilon_1/T)$ cm$^3$ s$^{-1}$,
$\varepsilon_1 = 3050/R$ K (linear chain branching)[23,24]
($Q_1$ = 17 kcal mol$^{-1}$ and $Q_2$ = 34 kcal mol$^{-1}$);[3]

$NCl_2 + NCl_2 \rightarrow N_2 + Cl_2\ ^3\Pi_o{}^+{}_u + 2Cl$,
$k_3 = 6.0\times10^{-13}$ cm$^3$ s$^{-1}$ (nonlinear chain branching)[1,5]

$Cl_2\ ^3\Pi_o{}^+{}_u \rightarrow 2Cl$,
$k_4 = 4.8\times10^2$ s$^{-1}$ (refs. 2, 25)

$Cl_2\ ^3\Pi_o{}^+{}_u + NCl_3 \rightarrow NCl_2 + Cl_2 + Cl$,
$k_5 = 1.6\times10^{-12}$ cm$^3$ s$^{-1}$ (ref. 1)

$Cl_2\ ^3\Pi_o{}^+{}_u + Cl \rightarrow Cl_2\ ^1\Sigma_g{}^+ + Cl$,
$k_6 = 1.6\times10^{-10}$ cm$^3$ s$^{-1}$ (nonlinear chain termination),[25]

$NCl_2 \rightarrow$ wall,
$k_7$ (heterogeneous chain termination in the diffusion-controlled region),

$Cl \rightarrow$ wall,
$k_8$ (heterogeneous chain termination in the diffusion-controlled region),

$Cl_2\ ^3\Pi_o{}^+{}_u + M \rightarrow Cl_2\ ^1\Sigma_g{}^+ + M$,
$k_9 = 10^{-13}$ cm$^3$ s$^{-1}$ in He, $9\times10^{-13}$ cm$^3$ s$^{-1}$ in $H_2$ (deactivation)[3,26]

$Cl + H_2 \rightarrow H + HCl$,
$k_{10} = 0.4\times10^{-11}\exp(-\varepsilon_2/T)$ cm$^3$ s$^{-1}$, $\varepsilon_2 = 2100/R$ K[27]

$H + Cl_2 \rightarrow Cl + HCl + Q_3$ (43 kcal mol$^{-1}$),
$k_{11} = 0.92\times10^{-10}\exp(-\varepsilon_3/T)$ cm$^3$ s$^{-1}$, $\varepsilon_3 = 720/R$ K[27,†]

$H + NCl_3 \rightarrow NCl_2 + HCl$,
$k_{12} = 4.0\times10^{-12}$ cm$^3$ s$^{-1}$ (ref. 28);

$H + NCl_2 \rightarrow NCl + HCl$,
$k_{13} = 9.0\times10^{-11}$ cm$^3$ s$^{-1}$ (ref. 28);

$H + NCl_3 \rightarrow NHCl + 2Cl$,
$k_{14} \sim k_{12}$ (ref. 17) [the step of extra linear branching must occur because the promotion of $NCl_3$ self-ignition by $H_2$ was experimentally observed,[17] step (14) was taken from ref. 17, see below];

$H \rightarrow$ wall,
$k_{15}$ (heterogeneous chain termination in the diffusion-controlled region),

$Cl + NOCl \rightarrow NO + Cl_2$,
$k_{16} = 3.0\times10^{-11}$ cm$^3$ s$^{-1}$ (homogeneous chain termination).[29]

We assumed that heat resulted from reactions (1), (2) and (11). The following equation corresponds to a heat balance:[18]

$$q_0 = (Q_1[Cl][NCl_3]k_1 + Q_2[NCl_2][NCl_3]k_2 + Q_3[H][Cl_2]k_{11})/(C_p\rho) - \alpha L(T - 298)/(C_p\rho), \quad (1)$$

where $Q_1$ and $Q_2$ are the specific heats, $C_p$ is heat capacity ($C_p$ = 1.25 and 2 cal g$^{-1}$ K$^{-1}$ for the $NCl_3$–He and $NCl_3$–$H_2$ mixtures, respectively[19]), $\alpha$ is the heat-transfer coefficient, and $L$ is the surface area-to-volume ratio (cm$^{-1}$). $\alpha$ was estimated[3] from the relationship $\alpha = L\delta\lambda e/r^2$, where $r$ is the reactor radius (cm), $e$ is the Napierian base, $\delta$ = 2.0 is the critical parameter, and $\lambda$ is the heat conductivity of the mixture (which was taken equal to that of He in inhibition experiments and to that of hydrogen in promotion).

The problem is considered in a one-dimensional approximation. The characteristic scales of time, length and velocity, as well as dimensionless variables and parameters, were chosen as described previously:[2,3]

$\tau = k_1[NCl_3]_0 t$, $Y_0 = [Cl]/[NCl_3]_0$, $Y_1 = [Cl_2\ 3\Pi_o{}^+{}_u]/[NCl_3]_0$,
$Y_2 = [NCl_2]/[NCl_3]_0$, $Y_3 = [NCl_3]/[NCl_3]_0$, $\beta = k_2/k_1$,
$\phi = k_3/k_1$, $\gamma = k_8/(k_1[NCl_3]_0)$, $\lambda = k_4/(k_1[NCl_3]_0)$,
$\psi = k_5/k_1$, $\rho = k_7/(k_1[NCl_3]_0)$, $\mu = k_6/k_1$,
$\chi = k_9/(k_1[NCl_3]_0)$.

$t$ is time (s), the dimensionless velocity and coordinate of the propagating flame were defined in terms of the diffusivity of $NCl_3$ ($D_3$): $\varpi = U/(D_3k_1[NCl_3]_0)^{1/2}$, $\xi = x/(D_3/k_1[NCl_3]_0)^{1/2}$, where $U$ and $x$ are the corresponding dimensional values. Let us define the dimensionless diffusion coefficients of chlorine atoms – $D_0$, $Cl_2\ ^3\Pi_o{}^+{}_u$ – $D_1$, $NCl_2$ – $D_2$, H atoms – $D_5$, NOCl – $D_6$, $Cl_2$ – $D_7$, as $\delta_0$, $\delta_1$, $\delta_2$, $\delta_5$, $\delta_6$ and $\delta_7$, respectively. Additional variables were introduced:

$Y_5 = [H]/[NCl_3]_0$, $Y_6 = [NOCl]/[NCl_3]_0$, $Y_7 = [Cl_2]/[NCl_3]$,
$\eta = k_7/(k_1[NCl_3]_0)$, $\gamma = k_8/(k_1[NCl_3]_0)$, $k = k_{10}/k_1$,
$\pi = k_{11}/k_1$, $\theta = k_{12}/k_1$, $\zeta = k_{13}/k_1$,
$\nu = k_{15}/(k_1[NCl_3]_0)$, $\sigma = k_{16}/k_1$.

Note that $Y_4$ is temperature (K). The mole fraction of NOCl in the mixture will be designated as v. Dimensionless thermal diffusivity is $\delta_4 = D/D_3$, where $D$ is dimensional thermal diffusivity, which was taken equal to the self-diffusion coefficient of He (1.62 cm$^2$ s$^{-1}$ under normal conditions[19]).

Thus, we arrive at the following set of second-order partial differential diffusion-kinetic equations:

† The reverse of step (10) does not affect the calculated data.

$$\partial Y_0/\partial\tau = \delta_0\ \partial^2 Y_0/\partial\xi^2 + 2\phi(Y_2)^2 + \psi Y_1 Y_3 + 2\lambda Y_1 - Y_0 Y_3 + 3Y_2 Y_3\beta \exp(-\varepsilon_1/Y_4) - \kappa Y_0 \exp(-\varepsilon_2/Y_4)/s + 2\theta Y_3 Y_5 - \sigma Y_0 Y_6 \mathrm{v}/s - \gamma Y_0$$

$$\partial Y_1/\partial\tau = \delta_1\ \partial^2 Y_1/\partial\xi^2 + 2\phi(Y_2)^2 - \psi Y_1 Y_3 - \lambda Y_1 - \chi P Y_1 - \mu Y_0 Y_1 \qquad \text{(I)}$$

$$\partial Y_2/\partial\tau = \delta_2\ \partial^2 Y_2/\partial\xi^2 - 2\phi(Y_2)^2 + \psi Y_1 Y_3 - \eta Y_2 - Y_2 Y_3\beta \exp(-\varepsilon_1/Y_4) + \theta Y_3 Y_5 - \zeta Y_2 Y_5 + Y_0 Y_3$$

$$\partial Y_3/\partial\tau = \partial^2 Y_3/\partial\xi^2 - \psi Y_1 Y_3 - Y_0 Y_3 - Y_2 Y_3\beta \exp(-\varepsilon_1/Y_4) - 2\theta Y_3 Y_5$$

$$\partial Y_4/\partial\tau = \delta_4\ \partial^2 Y_4/\partial\xi^2 + 3.8\times10^{-5} s[Q_2 Y_2 Y_3\beta \exp(-\varepsilon_1/Y_4) + Q_3\pi Y_5 Y_7 \exp(-\varepsilon_3/Y_4) + Q_1 Y_0 Y_3]/(C_\mathrm{p}\rho) - 10^{-6}(Y_4 - 298)/(sC_\mathrm{p}\rho P^2)$$

$$\partial Y_5/\partial\tau = \delta_5\ \partial^2 Y_5/\partial\xi^2 - 2\theta Y_3 Y_5 + \kappa Y_0 \exp(-\varepsilon_2/Y_4)/\mathrm{s} - \nu Y_5 - \zeta Y_2 Y_5$$

$$\partial Y_6/\partial\tau = \delta_6\ \partial^2 Y_6/\partial\xi^2 - \sigma Y_0 Y_6 \mathrm{v}/s$$

$$\partial Y_7/\partial\tau = \delta_1\ \partial^2 Y_7/\partial\xi^2 + \mu Y_0 Y_1 + \psi Y_1 Y_3 + 2\lambda Y_1 + Y_0 Y_3 + \chi P Y_1 + Y_2 Y_3\beta \exp(-\varepsilon_1/Y_4) - \pi Y_0 \exp(-\varepsilon_3/Y_4)$$

The solutions to set (I) satisfy the following boundary conditions for flame propagating from the right to the left:[2,3]

$$Y_0, Y_1, Y_2, Y_4, Y_5 \to 0,\ \xi \to \pm\infty \qquad \text{(II)}$$

$$Y_3 \to 1,\ \xi \to -\infty;\quad Y_3 \to 0,\ \xi \to +\infty;\quad Y_6 \to \mathrm{v}/s,\ \xi \to -\infty.$$

The chain-initiation reaction is ignored.[15] Based on experimental data, we simulated the inhibition of an isothermal flame and flame promotion (in the former case, the reactions involving H and $H_2$ were excluded from set (I); in the latter case, the reactions involving NOCl were excluded). The set of equations (I) was solved numerically.[3] Since heterogeneous chain termination was considered to occur in the diffusion-controlled region, the rate constants $k_7$, $k_8$ and $k_{14}$ were calculated[3] using the $D_i$ values of the reaction mixture components.[3,16] The procedure for determining the autoignition limits is described below.[30] The deviation of concentration $Y_1$ from its stationary values can be expressed as $Y_1 - Y_{1\mathrm{st}} = A_1\exp\omega_1 t + A_2\exp\omega_2 t + A_3\exp\omega_3 t + A_4\exp\omega_4 t$, where $A_i$ are constants. Let this be true for the other $Y_i$. The exponents are defined by the eigenvalues of the following matrix (note that the elements of this matrix contain only terms corresponding to the reaction intermediates and to the elementary reactions that are linear with respect to these intermediates):

$$\begin{vmatrix} \partial/\partial[Y_0](\mathrm{d}Y_0/\mathrm{d}\tau) - \omega & \partial/\partial Y_1(\mathrm{d}Y_0/\mathrm{d}\tau) & \partial/\partial Y_3(\mathrm{d}Y_0/\mathrm{d}\tau) & \partial/\partial Y_5(\mathrm{d}Y_0/\mathrm{d}\tau) \\ \partial/\partial[Y_0](\mathrm{d}Y_1/\mathrm{d}\tau) & \partial/\partial \mathrm{Y}_1(\mathrm{d}Y_1/\mathrm{d}\tau) - \omega & \partial/\partial Y_3(\mathrm{d}Y_1/\mathrm{d}\tau) & \partial/\partial Y_5(\mathrm{d}Y_1/\mathrm{d}\tau) \\ \partial/\partial[Y_0](\mathrm{d}Y_2/\mathrm{d}\tau) & \partial/\partial Y_1(\mathrm{d}Y_2/\mathrm{d}\tau) & \partial/\partial Y_3(\mathrm{d}Y_2/\mathrm{d}\tau) - \omega & \partial/\partial Y_5(\mathrm{d}Y_2/\mathrm{d}\tau) \\ \partial/\partial[Y_0](\mathrm{d}Y_5/\mathrm{d}\tau) & \partial/\partial Y_1(\mathrm{d}Y_5/\mathrm{d}\tau) & \partial/\partial Y_3(\mathrm{d}Y_5/\mathrm{d}\tau) & \partial/\partial Y_5(\mathrm{d}Y_5/\mathrm{d}\tau) - \omega \end{vmatrix} = 0 \qquad (2)$$

Matrix (2) is equivalent to the equation $\omega^4 + A\omega^3 + B\omega^2 + C\omega + D = 0$. Coefficients $A$, $B$, and $C$ have a constant sign for the above kinetic scheme. Coefficient $D$, which is the determinant of matrix (2), changes its sign. When this happens, at least one of the exponents infinitely grows, implying ignition. By equating determinant (2) to zero, we define a curve that is a boundary of the autoignition region on the ($P$, $T$) plane. Because termolecular chain termination was ignored in our calculations,[2] we determined only the lower autoignition limit. Figure 1 presents the results of a numerical simulation of the inhibition of IFP (thick lines). These results were obtained for $k_{16} = 1.4\times10^{-11}$ cm$^3$ s$^{-1}$. We can judge only qualitative agreement between the calculated and observed data. It was not our aim to fit the calculated flame velocities and IFP limits to experimental data by varying constants $k_i$. This fitting would be of a low value because a large number of parameters would be introduced in the calculation. This is also true of step (14); the establishment of the chemical nature of the extra linear branching step calls for further investigation. However, the observed decrease in the flame velocity and the narrowing of the IFP region, caused by an increase in the inhibitor concentration in a combustible mixture, is qualitatively predicted by set (I). Figure 2(*a*) presents calculated data that illustrate the promotion of an IFP flame. A comparison between the calculated and experimental data confirms that flame propagation in the 0.5% $NCl_3 + H_2$ mixture is isothermal. Both experiments and calculations suggest that IFP occurs outside the autoignition region (see above). Furthermore, calculated data [Figure 2(*a*), thin line] demonstrate that raising the diffusion coefficients of the intermediates in $H_2$ without allowing for promotion will not fit the calculated data to the observed data. Therefore, the IFP velocity in $H_2$ is higher than that in He owing to $H_2$ promoting $NCl_3$ decomposition [Figure 2(*b*)]. As demonstrated for the reaction between $NCl_3$ and $H_2$ near the lower autoignition limit,[17] reaction (10) is a link between $NCl_3$ decomposition and additional branching reaction (14) (promotion).

Thus, we analysed experimental data on the inhibition and promotion of IFP for $NCl_3$ decomposition in helium in the presence of NOCl (inhibitor) and $H_2$ (promoter). We performed a numerical simulation of this process taking into account energy chain branching. The results are in qualitative agreement with experimental data. Based on previous data[1–3] and this work, the reaction near the lower self-ignition limit can be considered as a model nonlinear BCP.

We thank Professor V. V. Azatyan for helpful discussions. This work was supported by the Russian Foundation for Basic Research (grant nos. 00-03-32979a and 02-03-32993a).

## References

1 N. M. Rubtsov, *Mendeleev Commun*., 1998, 173.
2 N. M. Rubtsov and V. D. Kotelkin, *Mendeleev Commun*., 2001, 61.
3 N. M. Rubtsov and V. D. Kotelkin, *Mendeleev Commun.*, 2002, 33.
4 N. N. Semenov, *O nekotorych problemakh khimicheskoi kinetiki i reaktsionnoi sposobnosti* (*On Some Problems of Chemical Kinetics and Reaction Ability*), Academy of Sciences of the USSR, Moscow, 1968, p. 686 (in Russian).
5 V. V. Azatyan, R. R. Borodulin and N. M. Rubtsov, *Dokl. Akad. Nauk SSSR*, 1979, **249**, 1375 [*Dokl. Chem*. (*Engl.Transl.*), 1979, **249**, 1265].
6 V. V. Azatyan, R. R. Borodulin and N. M. Rubtsov, *Fiz. Goren. Vzr.*, 1980, **5**, 34 (in Russian).
7 N. M. Rubtsov, *Kinet. Katal*., 2000, **41**, 12 [*Kinet. Catal*. (*Engl. Transl*.), 2000, **41**, 11].
8 V. V. Azatyan, R. R. Borodulin, E. A. Markevich, N. M. Rubtsov and N. N. Semenov, *Izv. Akad. Nauk SSSR, Ser. Khim*., 1976, 1459 (*Bull. Acad. Sci. USSR, Div. Chem. Sci*., 1980, **29**, 1165).
9 V. V. Azatyan, R. R. Borodulin and N. M. Rubtsov, *Kinet. Katal*., 1980, **21**, 316 [*Kinet. Catal*. (*Engl. Transl*.), 1980, **21**, 41].
10 A. A. Krasheninnikova, L. A. Furman and G. S. Ul'yankina, *Zh. Prikl. Khim.*, 1971, **44**, 2183 [*J. Appl. Chem. USSR* (*Engl. Transl.*), 1971, **44**, 2232].
11 F. Baillou, R. Lisbet and G. Dupre, *Proceedings of the 7th Int. Symp. on Loss Prevention and Safety Promotion in the Process Industries*, Taormine, 1992, p. 43.
12 V. V. Azatyan, *Kinet. Katal*., 1999, **40**, 818 [*Kinet. Catal*. (*Engl. Transl*.), 1999, **40**, 720].
13 T. L. Hersuaw, S. D. Herrero and L. A. Schlie, *J. Phys. Chem*., 1998, **102**, 6239.
14 N. M. Rubtsov, Dr. Sci. Thesis, Institute for Structural Macrokinetics RAS, Chernogolovka, 1997, p. 350 (in Russian).
15 Z. I. Kaganova, Ph. D. Thesis, Institute of Chemical Physics RAS, Moscow, 1982, p. 162 (in Russian).
16 Z. I. Kaganova and B. V. Novozhilov, *Khim. Fiz.*, 1982, 1213 (in Russian).
17 N. M. Rubtsov, *Kinet. Katal*., 2001, **42**, 626 [*Kinet. Catal*. (*Engl. Transl*.), 2001, **42**, 541].
18 D. A. Frank-Kamenetskii, *Diffuziya i teploperedacha v khimicheskoi kinetike* (*Diffusion and Heat Transfer in Chemical Kinetics*), Nauka, Moscow, 1967 (in Russian).
19 *Tablitsy fizicheskikh velichin* (*Tables of Physical Quantities*), ed. I. K. Kikoin, Atomizdat, Moscow, 1976, p. 112 (in Russian).
20 T. C. Clark and M. A. A. Clyne, *J. Chem. Soc., Faraday Trans*., 1970, **66**, 372.
21 V. V. Azatyan, R. R. Borodulin, E. A. Markevich and N. M. Rubtsov, *Fiz. Goren. Vzr.*, 1978, **2**, 20 (in Russian).
22 M. M. Rubtsov, V. V. Azatyan and R. R. Borodulin, *Izv. Akad. Nauk SSSR, Ser. Khim*., 1980, 1234 (*Bull. Acad. Sci. USSR, Div. Chem. Sci.*, 1980, **29**, 860).
23 V. V. Azatyan, R. R. Borodulin, E. A. Markevich, N. M. Rubtsov and N. N. Semenov, *Dokl. Akad. Nauk SSSR*, 1975, **224**, 1096 [*Dokl. Chem*. (*Engl. Transl*.), 1975, **224**, 1065].
24 N. M. Rubtsov and R. R. Borodulin, in *Kinetika i mekhanizm fiziko-khimicheskikh protsessov* (*Kinetics and Mechanisms of Physico-chemical Processes*), ed. S. A. Tsyganov, Institute of Chemical Physics, Chernogolovka, 1981, p. 14 (in Russian).

25 M. A. A. Clyne and D. H. Stedman, *J. Chem. Soc., Faraday Trans*., 1968, **64**, 2698.
26 T. C. Clark and M. A. A. Clyne, *J. Chem. Soc., Faraday Trans*., 1970, **66**, 372.
27 P. F. Ambidge, J. N. Bradley and D. A. Whittock, *J. Chem. Soc., Faraday Trans*., 1976, **72**, 2143.
28 D. B. Exton, J. V. Gilbert and R. D. Coombe, *J. Phys. Chem*., 1991, **95**, 2692.
29 M. A. A. Clark and H. W. Cruse, *J. Chem. Soc., Faraday Trans*., 1972, **68**, 1281.
30 P. Gray, J. F. Griffiths and S. K. Scott, *Proc. R. Soc. London*, 1985, **402**, 187.

*Received: 5th July 2002; Com. 02/1956*